

Ventilation procedures to minimize the airborne transmission of viruses at schools

— [Source link](#) 

Luca Stabile, Antonio Pacitto, A. Mikszewski, Lidia Morawska ...+2 more authors

Institutions: University of Cassino, Queensland University of Technology

Published on: 24 Mar 2021 - medRxiv (Cold Spring Harbor Laboratory Press)

Topics: Airborne transmission

Related papers:

- [Assessment of Airborne Disease Transmission Risk and Energy Impact of HVAC Mitigation Strategies](#)
- [Beyond Six Feet: A Guideline to Limit Indoor Airborne Transmission of COVID-19](#)
- [Quantifying the Tradeoff Between Energy Consumption and the Risk of Airborne Disease Transmission for Building HVAC Systems](#)
- [Mitigating COVID-19 infection disease transmission in indoor environment using physical barriers](#)
- [The prediction of airflow regimes in surgical operating theatres: a comparison of different turbulence models](#)

Share this paper:    

View more about this paper here: <https://typeset.io/papers/ventilation-procedures-to-minimize-the-airborne-transmission-3cxrax0dep>

Ventilation procedures to minimize the airborne transmission of viruses at schools

L. Stabile^{1,*}, A. Pacitto¹, A. Mikszewski², L. Morawska², G. Buonanno^{1,2}

¹ Department of Civil and Mechanical Engineering, University of Cassino and Southern Lazio, Cassino, FR, Italy

² International Laboratory for Air Quality and Health, Queensland University of Technology, Brisbane, Qld, Australia

*Corresponding author:

Luca Stabile

Department of Civil and Mechanical Engineering,

University of Cassino and Southern Lazio, Cassino, FR, Italy

l.stabile@unicas.it

Abstract

Reducing the transmission of SARS-CoV-2 through indoor air is the key challenge of the COVID-19 pandemic. Crowded indoor environments, such as schools, represent possible hotspots for virus transmission since the basic non-pharmaceutical mitigation measures applied so far (e.g. social distancing) do not eliminate the airborne transmission mode. There is widespread consensus that improved ventilation is needed to minimize the transmission potential of airborne viruses in schools, whether through mechanical systems or *ad-hoc* manual airing procedures in naturally ventilated buildings. However, there remains significant uncertainty surrounding exactly what ventilation rates are required, and how to best achieve these targets with limited time and resources. This paper uses a mass balance approach to quantify the ability of both mechanical ventilation and *ad-hoc* airing procedures to mitigate airborne transmission risk in the classroom environment. For naturally-ventilated classrooms, we propose a novel feedback control strategy using CO₂ concentrations to continuously monitor and adjust the airing procedure. Our case studies show how such procedures can be applied in the real world to support the reopening of schools during the pandemic. Our results also show the inadequacy of relying on absolute CO₂ concentration thresholds as the sole indicator of airborne transmission risk.

Keywords: exhaled CO₂; virus transmission; air exchange rate; ventilation; schools; SARS-CoV-2.

1 Introduction

The COVID-19 pandemic caused by the novel SARS-CoV-2 virus has put indoor environments in the spotlight since they are where virus transmission predominately occurs [1–4]. Indeed, insufficient ventilation in highly crowded environments such as restaurants, schools, and gyms does not allow proper dilution of virus-laden respiratory particles emitted by infected subjects, leading to a high percentage of secondary infections amongst exposed susceptibles [2,5–8]. To this end, governments worldwide have imposed temporary shutdowns of most indoor environments, including schools [9–14], being in the difficult role of deciding whether to prioritize the right to education or to health. After the first pandemic wave (early 2020), guidelines for reopening schools were prepared and adopted in view of opening the schools in the late (northern hemisphere) summer, but they mainly relied upon promoting personal behaviors and basic non-pharmaceutical mitigation measures (i.e. social distancing, hand washing, wearing masks) that address close contact transmission [15], which is a minor route of transmission in indoor environments if a social distance is guaranteed [16,17]. The limited effect of such measures was confirmed by a resurgence of the virus in late 2020 that caused

51 schools to close once more in many countries worldwide [18,19]
52 (en.unesco.org/covid19/educationresponse). Thus, in order to open schools safely at the time of
53 pandemics, airborne transmission related to the small airborne respiratory particles (droplet nuclei)
54 [15] needs to be taken into account since it is potentially the dominant mode of transmission of
55 numerous respiratory infections, including SARS-CoV-2 [3,20–23]; therefore, while waiting for the
56 vaccination campaign to be completed, a suitable solution to minimize the virus transmission potential
57 in schools is providing *ad-hoc* ventilation able to lower the virus concentration indoors [6,8,24,25].
58 The provision of a proper ventilation rate certainly cannot be taken for granted since most of the
59 schools worldwide rely upon natural ventilation and manual airing (e.g. 86% of the European school
60 buildings investigated within the SINPHONIE project [26,27]). For such schools, a potential approach
61 to monitor and minimize the virus spread in indoor environments could be the use of a proxy
62 providing real-time information on the virus concentration indoors then suggesting to apply manual
63 ventilation procedures accordingly. Exhaled CO₂ has been proposed as a possible proxy for virus
64 transmission indoors as it is a commonly used indicator of the ventilation rate and, more generally,
65 indoor air quality [28–30]. While in principle exhaled CO₂ could be a good proxy for indoor-generated
66 gaseous pollutants (e.g. VOCs, radon) [31], it cannot predict behaviors and dynamics of virus-laden
67 particles which are affected by phenomena typical of all airborne particles such as deposition, and
68 filtration (if any) in addition to virus inactivation. As such, the best application of exhaled CO₂ is
69 estimating the air exchange rate of confined spaces [32,33]. Indeed, if the particle deposition rate and
70 virus inactivation rate are known, the indoor virus concentration is just affected by the air exchange
71 rate; with this in mind, exhaled CO₂ can predict the virus spreading in indoor environments and CO₂
72 sensors can represent a marker of the corresponding infection risk [24,29,34,35]. Nonetheless, at this
73 stage of the scientific debate, the question is not just demonstrating the qualitative association
74 between ventilation (or CO₂ levels) in buildings and the transmission of infectious diseases
75 [3,6,8,24,28,36,37], but quantifying and guaranteeing the required ventilation in highly crowded
76 environments (e.g. schools) to reduce the spread of infectious diseases via airborne route whether
77 mechanical ventilation systems are installed or not.
78 In the present paper we evaluated the required air exchange rates for mechanically-ventilated schools
79 and adequate airing procedures for naturally-ventilated schools to reduce the transmission potential
80 of a respiratory virus (expressed as reproduction number) through the airborne route of transmission.
81 Moreover, a suitable feedback control strategy, based on the continuous measurement of the indoor
82 exhaled CO₂ concentration, was proposed to monitor that an acceptable individual risk of infection is
83 continuously maintained even in schools not equipped with mechanical ventilation systems. To this
84 end, simulations based on virus and exhaled CO₂ mass balance equations considering typical school
85 scenarios were performed.

86 **2 Materials and methods**

87 The required air exchange rates and the adequate airing procedures to maintain an acceptable level of
88 the virus transmission risk were calculated adopting the virus and CO₂ mass balance equations
89 (described in section 2.1 and 2.2) under the simplified hypothesis that they are both instantaneously
90 and evenly distributed in the confined space under investigation (box-model). Here particle
91 deposition and virus inactivation phenomena were taken into account and dynamic scenarios
92 (described in section 2.3) have been simulated within the 5-hour school-day. Two different viruses,
93 characterized by extremely different emission rates (i.e. different viral loads and infectious doses)
94 [38], were considered: SARS-CoV-2 and seasonal influenza. The study involves infected people
95 breathing and/or speaking whereas severely symptomatic persons frequently coughing or sneezing
96 were not included in the scenarios. The simulations were performed under the hypothesis that the
97 students are adequately spaced so that ballistic deposition of large respiratory particles (> 100 μm)
98 onto mucous membranes is considered negligible [15]; thus, virus transmission results solely from the
99 Inhalation of airborne particles (i.e. airborne transmission).

100 **2.1 Evaluation of the virus transmission potential**

101 The virus transmission potential due to the airborne route was assessed in terms of event
102 reproduction number (R_{event}) which is the expected number of new infections arising from a single

103 infectious individual at a specific event [39] (e.g. a single school day). In particular, the R_{event} was
104 evaluated adopting the approach proposed and applied in previous papers [5,6,40]; involving six
105 successive steps: (i) the quanta emission rate, (ii) the exposure to quanta concentration in the
106 microenvironment, (iii) the dose of quanta received by exposed susceptible subjects, (iv) the
107 probability of infection on the basis of a dose-response model, (v) the individual risk of the exposed
108 person, and, finally, (vi) the event reproduction number. The above-mentioned “quanta” is a measure
109 to quantify the virus emission or concentration, it is defined as the infectious dose for 63% of
110 susceptibles by inhalation of virus-laden particles. In particular, the evaluation of the quanta emission
111 rate (ER_q , quanta h^{-1}) was described in our previous papers taking into account the viral load,
112 infectious dose, respiratory activity, activity level, and particle volume concentration expelled by the
113 infectious person [5,6,38]. The model, here not reported for the sake of brevity, provides a distribution
114 of quanta emission rates, i.e. the probability density function of ER_q . It represents a major step forward
115 to properly simulate and predict infection risk in different indoor environments via airborne
116 transmission since previous studies were performed adopting quanta emission rates obtained from
117 rough estimates based on retrospective assessments of infectious outbreaks only at the end of an
118 epidemic [24,41]. The predictive approach also enables stochastic analysis of infection probability that
119 is not possible when using a point estimate obtained from a superspreading event.
120 The indoor quanta concentration over time, $n(t, ER_q)$, is evaluated, for each possible ER_q value,
121 adopting the above-mentioned simplified mass balance equation as:

$$122 \quad n(t, ER_q) = n_0 \cdot e^{-(AER+k+\lambda) \cdot t} + \frac{ER_q \cdot I}{(AER+k+\lambda) \cdot V} \cdot (1 - e^{-(AER+k+\lambda) \cdot t}) \quad (\text{quanta } m^{-3}) \quad (1)$$

124 where AER (h^{-1}) is the air exchange rate, k (h^{-1}) is the deposition rate on surfaces, λ (h^{-1}) is the viral
125 inactivation rate, I is the number of infectious subjects, and V is the volume of the indoor environment.
126 The dose of quanta (D_q) received by a susceptible subject exposed to a certain quanta concentration
127 for a certain time interval, T , can be evaluated by integrating the quanta concentration over time as:

$$128 \quad D_q(ER_q) = IR \int_0^T n(t, ER_q) dt \quad (\text{quanta}) \quad (2)$$

130 where IR is the inhalation rate of the exposed subject which is a function of the subject’s activity level
131 and age [42,43].

132 The probability of infection (P_I , %) of exposed persons (for a certain ER_q), is evaluated on the basis of
133 simple Poisson dose-response model [44,45] as:

$$134 \quad P_I(ER_q) = 1 - e^{-D_q(ER_q)} \quad (\%) \quad (3)$$

135 The individual risk of infection (R) of an exposed person for a given exposure scenario is then
136 calculated integrating, over for all the possible ER_q values, the product between the conditional
137 probability of the infection for each ER_q ($P_I(ER_q)$) and the probability of occurrence of each ER_q value
138 (P_{ER_q}):

$$139 \quad R = \int_{ER_q} (P_I(ER_q) \cdot P_{ER_q}) dER_q \quad (\%) \quad (4)$$

140 Such an individual risk R , for a given exposure scenario, represents the ratio between the number of
141 new infections (number of cases, C) and the number of exposed susceptible individuals (S). The R_{event}
142 (expected number of new infections, C , arising from a single infectious individual, I , at a specific event)
143 can be obtained as the product of R and S :

$$144 \quad R_{event} = R \cdot S \quad (\text{infections}) \quad (5)$$

145 Therefore, the maximum number of susceptibles that can stay simultaneously in the confined space
146 under investigation for an acceptable $R_{event} < 1$ (hereinafter referred as maximum room occupancy,
147 MRO) is:

156
157 $MRO < 1/R$ (susceptibles) (6)

158 2.2 Evaluation of the CO₂ indoor levels

159 To estimate the trend of indoor (exhaled) CO₂ concentration over time (CO_{2-in}) a mass balance
160 equation was applied considering the initial indoor CO₂ concentration (at t=0) equal to outdoor air
161 (CO_{2-out}), the mass balance equation can be simplified as [32]:

162
163 $CO_{2-in}(t) = CO_{2-out} + \frac{ER}{V \cdot AER} \cdot (1 - e^{-AER \cdot t})$ (ppm) (7)

164
165 where ER represents the overall exhaled CO₂ emission rate in the indoor environment under
166 investigation; the emission rate per-capita are available in the scientific literature (typically expressed
167 in L s⁻¹ person⁻¹) as a function of the activity level, age, and gender [46]. As mentioned above, for
168 known and steady state emission rate and outdoor CO₂ concentration, the indoor concentration is just
169 affected by the air exchange rate of the room, and the AER can be back-calculated from the eq. 7
170 measuring continuously the indoor CO₂ concentration (CO_{2-in}): this measurement method is known as
171 “constant injection rate method” [32,47].

172 2.3 Simulated scenarios

173 The individual risk of infection and the event reproduction number of a disease due to the airborne
174 transmission route of the virus were assessed considering a high-school classroom (e.g. students aged
175 17-18) with a floor area of 50 m² and a height of 3 m (V=150 m³). A crowding index suggested by the
176 standard EN 15251 [48] on the design of the ventilation for a proper indoor air quality (2 m² person⁻¹)
177 was adopted then obtaining a total number of occupants (including the teacher) of 25 persons. A total
178 school-time of 5 hours was considered. The simulations were performed considering one infected
179 subject (I=1), the teacher or one of the students, and 24 exposed susceptibles (S=24) hypothesizing
180 that none of them is already immune (e.g. vaccinated). Therefore, in order to obtain a R_{event} < 1, the
181 individual risk of infection (R) of the exposed susceptible over the 5-hour school-time should be less
182 than 1/24, i.e. < 4.2%.

183 The simulations were conducted for different scenarios, i.e. combination of emitting subject and
184 mitigation solution (if any). Two different emitting subjects were considered in the simulation: the
185 teacher and the student. In particular, simulations were performed considering (a) the infected
186 teacher giving lesson (i.e. speaking or loudly speaking) for one hour, in particular, the first hour of
187 lesson was considered as it is clearly the worst exposure scenario for susceptible students attending
188 the lesson (in fact, the latest the infected teacher enters the classroom, the shorter the exposure period
189 of the susceptible persons), or (b) the infected student attending lessons, then just breathing, and/or
190 speaking occasionally. The exposed susceptibles were considered performing activities in a sitting
191 position then inhaling at IR = 0.54 m³ h⁻¹ [42,43].

192 The emitting scenarios are summarized in Table 1, whereas the corresponding quanta emission rate
193 probability distribution function for SARS-CoV-2 and seasonal influenza viruses, as a function of
194 activity level (i.e. sitting) and respiratory activity, are summarized in Table 2 as obtained from
195 previous papers [5,6]. The ER_q clearly increases for more severe respiratory activities, e.g. the median
196 SARS-CoV-2 ER_q ranges from 0.575 quanta h⁻¹ for oral breathing to 15.85 quanta h⁻¹ for loudly
197 speaking. Moreover, due to its higher infectious dose (i.e. RNA copies to reach a quanta), for similar
198 activity levels and respiratory activities, the SARS-CoV-2 ER_q values were much higher than the
199 seasonal influenza ones [5,38,49–51] (e.g. more than 10-fold at median value).

200 Despite the base scenarios, as summarized in Table 1, the possible effects of infected student’s
201 speaking duration (10% to 40% of the time), class duration (school hour of 55, 50, 45, or 40 min
202 instead of 60 min), infected teacher’s voice modulation (e.g. using microphone), and wearing mask
203 were considered in the simulations and described in detail. The effect of the mask was simulated
204 considering an overall 40% reduction of the dose of quanta received by the susceptibles [52], to this
205 end, in such simulations the ER_q values were halved.

206 The emission rate of exhaled CO₂ was evaluated considering a per-capita emission rate equal to
207 0.0044 L s⁻¹ person⁻¹ as an average value between males and female teenager students (e.g. aged 17-

208 18) with a level of physical activity of 1.3 met [46], which is the suggested level for reading, writing,
 209 typing in a sitting position at school. The overall emission rate (ER) was evaluated multiplying the per-
 210 capita emission rate by the number of student/teacher (25 person), then it resulted equal 0.110 L s⁻¹.
 211 In the simulations here proposed the outdoor CO₂ concentration (CO_{2-out}) was set at 500 ppm.

212 **Table 1** – Scenarios considered to simulate the exposure to SARS-CoV-2 and seasonal influenza viruses in the
 213 classroom: emitting subjects, emission duration, and respiratory activity are summarized (whereas the same
 214 activity level, i.e. sitting, was considered for all the scenarios). Descriptions of the base scenarios and of the
 215 possible mitigation solutions are reported.

Scenarios	Emitting subject	Emission duration (min), respiratory activity	Description	
Base scenarios	T-60-LS	teacher	60 min, loudly speaking	Infected teacher giving lesson for the first 60 min of the school-day loudly speaking
	S-0%-S	student	300 min, oral breathing	Infected student attending lessons for five hours (100% of the school-day) oral breathing
Student's speaking effect	S-10%-S	student	30 min, speaking & 270 min, oral breathing	Infected student attending lessons for 270 minutes (90% of the school-day) oral breathing and speaking for the rest of the time (10%)
	S-20%-S	student	60 min, speaking & 240 min, oral breathing	Infected student attending lessons for 240 minutes (80% of the school-day) oral breathing and speaking for the rest of the time (20%)
	S-30%-S	student	90 min, speaking & 210 min, oral breathing	Infected student attending lessons for 210 minutes (70% of the school-day) oral breathing and speaking for the rest of the time (30%)
	S-40%-S	student	120 min, speaking & 180 min, oral breathing	Infected student attending lessons for 180 minutes (60% of the school-day) oral breathing and speaking for the rest of the time (40%)
Class duration effect	T-55-LS	teacher	55 min, loudly speaking	Infected teacher giving lesson for the first 55 minutes of the school-day loudly speaking
	T-50-LS	teacher	50 min, loudly speaking	Infected teacher giving lesson for the first 50 minutes of the school-day loudly speaking
	T-45-LS	teacher	45 min, loudly speaking	Infected teacher giving lesson for the first 45 minutes of the school-day loudly speaking
	T-40-LS	teacher	40 min, loudly speaking	Infected teacher giving lesson for the first 40 minutes of the school-day loudly speaking
Voice modulation effect	T-60-S	teacher	60 min, speaking	Infected teacher giving lesson for the first 60 min of the school-day speaking (e.g. using a microphone)
Mask effect	T-60-LS-M	teacher	60 min, loudly speaking	Infected teacher giving lesson for the first 60 min of the school-day loudly speaking. Students and teacher wear a surgical mask.
Voice modulation & mask effect	T-60-S-M	teacher	60 min, speaking	Infected teacher giving lesson for the first 60 min of the school-day speaking (e.g. using a microphone). Students and teacher wear a surgical mask.

216

217 **Table 2** – Quanta emission rate distribution (ER_q, quanta h⁻¹), expressed as log₁₀ average and standard deviation
 218 values as well as 5th, 25th, 50th, 75th, and 95th percentiles, for SARS-CoV-2 and seasonal influenza viruses as a

219 function of respiratory activity. Virus inactivation rate, λ (h^{-1}), and particle deposition rate, k (h^{-1}) are also
 220 reported.

Respiratory activity	SARS-CoV-2			Seasonal influenza		
	Oral breathing	Speaking	Loudly speaking	Oral breathing	Speaking	Loudly speaking
$\log_{10}\text{ER}_q$ average $\log_{10}(\text{quanta h}^{-1})$	-0.240	0.410	1.200	-1.400	-0.770	0.064
$\log_{10}\text{ER}_q$ st. dev. $\log_{10}(\text{quanta h}^{-1})$	1.200	1.200	1.200	0.840	0.840	0.840
5th percentile (quanta h^{-1})	0.006	0.027	0.168	0.002	0.007	0.048
25th percentile (quanta h^{-1})	0.089	0.399	2.458	0.011	0.046	0.314
50th percentile (quanta h^{-1})	0.575	2.570	15.85	0.040	0.170	1.159
75th percentile (quanta h^{-1})	3.710	16.57	102.2	0.147	0.626	4.271
95th percentile (quanta h^{-1})	54.17	242.0	1492	0.959	4.090	27.91
Virus inactivation rate, λ (h^{-1})	0.63[53]			0.80[54]		
Particle deposition rate, k (h^{-1})	0.24[55]					

221 2.4 Required air exchange rates and airing procedures

222 The required air exchange rate to maintain a $R_{\text{event}} < 1$ in mechanically-ventilated schools for the
 223 abovementioned scenarios was calculated adopting the methodology described in section 2.1 and,
 224 especially, the eq. 1-5. Quanta emission rates were selected from Table 2 on the basis of the activity of
 225 the emitting subject (Table 1), the geometry of the classroom were reported in the section 2.3, the
 226 virus inactivation rate (λ) for SARS-CoV-2 (0.63 h^{-1}) [53] and seasonal influenza (0.80 h^{-1}) [54] as well
 227 as the particle deposition rate ($k=0.24 \text{ h}^{-1}$) [55] were obtained from the scientific literature and are
 228 summarized in Table 2. Having set these data, the individual risk of infection and, consequently, the
 229 event reproduction number, were just affected by the air exchange rate and the airing procedure of the
 230 classroom.

231 Quantifying the air exchange rate for mechanical ventilation systems is straightforward, as the fresh
 232 air ventilation rate can be easily measured in most cases, and should be consistent with the original
 233 design parameters of the system (assuming proper installation and routine maintenance).

234 For schools not equipped with mechanical ventilation systems, which are the majority [26,27], to
 235 maintain a $R_{\text{event}} < 1$, *ad-hoc* manual airing procedures based on manual airing cycles [31,56], i.e.
 236 adopting periods with windows closed and open alternatively, have to be determined. Indeed, unlike
 237 mechanical ventilation systems which are able to provide constant air exchange rate, the manual
 238 airing cycles will alternate periods at low air exchange rates (with window close) and periods at
 239 higher air exchange rates (with window open), and most importantly, such air exchange rates are not
 240 known *a priori*. Thus, for naturally-ventilated schools, an air exchange rate of the manual airing
 241 procedure can be calculated *a-posteriori* as school-day average resulting from the airing cycles (i.e.
 242 weighted average air exchange rate):

$$243 \quad AER = (AER_{NV} \cdot t_{NV} + AER_{MA} \cdot t_{MA}) / (t_{NV} + t_{MA}) \quad (8)$$

244 where AER_{NV} and AER_{MA} are the air exchange rates with window close (natural ventilation, NV) and
 245 window open (manual airing, MA), respectively, and t_{NV} and t_{MA} represent the total time during which
 246 the windows were kept closed and open, respectively; the sum of t_{NV} and t_{MA} clearly is the overall
 247 school time (i.e. 300 min). Since the air exchange rate is not constant all over the school day, the time
 248 at which the airing is adopted can significantly affect the quanta concentration trends. In fact, if a high
 249 quanta emission occurs when the windows are closed, the susceptibles could be exposed to high
 250 quanta concentrations then leading to a dose of quanta (and then an individual risk) larger than
 251 expected for a constant air exchange rate. In other words, for a certain exposure scenario, even when a
 252 school-day average AER provided with manual airing cycles is equal to the mechanical ventilation one,
 253 higher dose of quanta and individual risk can happen. Thus, in the case of manual airing cycles, higher
 254 average air exchange rates are needed to maintain a $R_{\text{event}} < 1$ with respect to classrooms equipped
 255

257 with mechanical ventilation systems, in particular for high but brief virus emissions. In our
258 simulations, the manual airing cycles were applied at the end of each school-hour (instead of at the
259 beginning of each lesson or between lessons), this just represents a constraint adopted in order to
260 limit the number of scenarios to be simulated, nonetheless, it does not undermine the findings and the
261 procedures we described.

262 Modeling air exchange rates from natural ventilation is extremely complex as leakages of the building
263 (AER_{NV}) and to the airing (AER_{MA}) are strongly influenced by the airtightness of the building and of the
264 windows, the wind conditions, the windows positioning within the classroom (single-sided vs. cross
265 ventilation), and the window opening angle [56–59]. As an example, previous papers [31,58]
266 performed experimental campaigns to measure the air exchange rate with window closed and opened
267 through a CO_2 decay method in classrooms and obtained significant variations of AER_{NV} ($< 0.3 h^{-1}$) and
268 AER_{MA} (up to $5 h^{-1}$). Summarizing, the ventilation rate via natural ventilation and manual airing is not
269 controlled; therefore, in view of maintaining a $R_{event} < 1$ a feedback mechanism (the indoor CO_2
270 concentration) is needed. We develop and apply this proper feedback control strategy to help optimize
271 *ad hoc* airing in classrooms.

272 3 Results and discussions

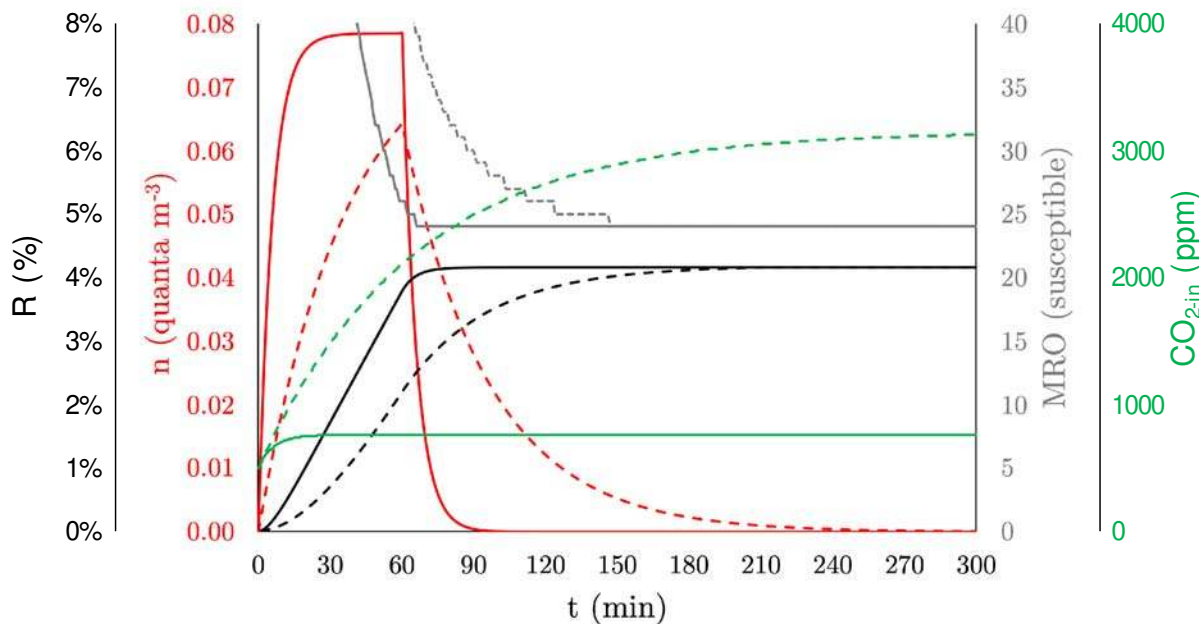
273 3.1 Required air exchange rates for mechanically-ventilated schools

274 Figure 1 presents the trends of quanta concentration, individual risk, Maximum Room Occupancy, and
275 indoor CO_2 concentration for the scenarios T-60-LS (teacher giving lesson loudly speaking for the first
276 60 min of the school-day) and T-60-S (i.e. speaking using a microphone instead of loudly speaking) in
277 the case of SARS-CoV-2 virus when required AERs (to maintain a $R_{event} < 1$) are provided through
278 mechanical ventilation systems. In particular, for the scenario T-60-LS, as summarized in Table 3, the
279 required AER is $9.5 h^{-1}$ (i.e. $> 15 L s^{-1} person^{-1}$). The quanta concentration trend increases sharply in
280 the first 60 min (i.e. when the virus source is still in the classroom), then exponentially decays as soon
281 as the teacher leaves the room and goes to zero at about 90 min. The individual risk reaches the
282 maximum permitted value (4.2%) at 90 min, then remaining constant up to the end of the school-day
283 (300 min) as we hypothesized that no other infected people enter the classroom. Similarly, as
284 designed, the maximum occupancy decreases to the needed value of 24 persons at the end of the
285 school-day. The authors point out that in the scenario T-60-LS the whole dose of quanta (and then
286 individual risk) is received by the susceptibles in roughly 90 minutes, thus, we would have designed
287 the same air exchange rate also in the hypothesis that the infected teacher gave a lesson at the second,
288 third or fourth hour. Due to the high (and constant) $AER = 9.5 h^{-1}$, the CO_2 indoor reaches the (very
289 low) equilibrium concentration of approximately 750 ppm in about half an hour.

290 For the scenario T-60-S, a much lower AER ($0.8 h^{-1}$; i.e. $1.3 L s^{-1} person^{-1}$) is required to maintain a
291 $R_{event} < 1$, indeed, the CO_2 indoor concentration does not even reach an equilibrium level and
292 continuously increases above 3000 ppm in five hours, which is well above the concentrations
293 suggested and obtainable if EN 15251 indoor air quality standards are adopted [48].

294 In Table 3 the required AERs to maintain a $R_{event} < 1$ for all the investigated scenarios are reported for
295 SARS-CoV-2 for mechanically-ventilated classrooms; the required AER for seasonal influenza-infected
296 subjects is not reported since it is $< 0.1 h^{-1}$ for all the scenarios under investigation. Thus, all the
297 ventilation techniques are able to protect against the spreading of the seasonal influenza virus in
298 classroom through airborne transmission. On the contrary, for SARS-CoV-2-infected subjects, the
299 required AERs can be quite high: as mentioned above, for a teacher giving lesson for one hour the
300 required AER is $9.5 h^{-1}$. Such AER can be reduced adopting shorter lessons (e.g. for 40-min lessons it
301 can decrease down to $6.1 h^{-1}$) or, even more, as discussed above, keeping the voice down while
302 speaking (e.g. using microphones, this would require just $0.8 h^{-1}$) and simultaneously wearing masks
303 (then lowering the required AER down to $0.2 h^{-1}$). If the infected subject is a student, an AER of $0.8 h^{-1}$
304 is needed if she/he does not speak for the entire school-day, then increasing for longer speaking
305 periods (e.g. $3.5 h^{-1}$ are required if she/he speaks for 40% of the school-day).

306



307
308
309
310
311
312
313

Figure 1 – Trends of quanta concentration (n), individual risk (R), Maximum Room Occupancy (MRO), and indoor CO_2 concentration (CO_{2-in}) resulting from the simulation of the base scenarios T-60-LS (infected teacher giving lesson loudly speaking for the first 60 min of the school day, solid lines) and T-60-S (infected teacher giving lesson speaking using a microphone for the first 60 min of the school day; dotted lines) in the case of SARS-CoV-2 virus having adopted the required constant AERs to maintain a $R_{event} < 1$ (9.5 h⁻¹ and 0.8 h⁻¹ for T-60-LS and T-60-S, respectively) through a mechanical ventilation system.

314
315

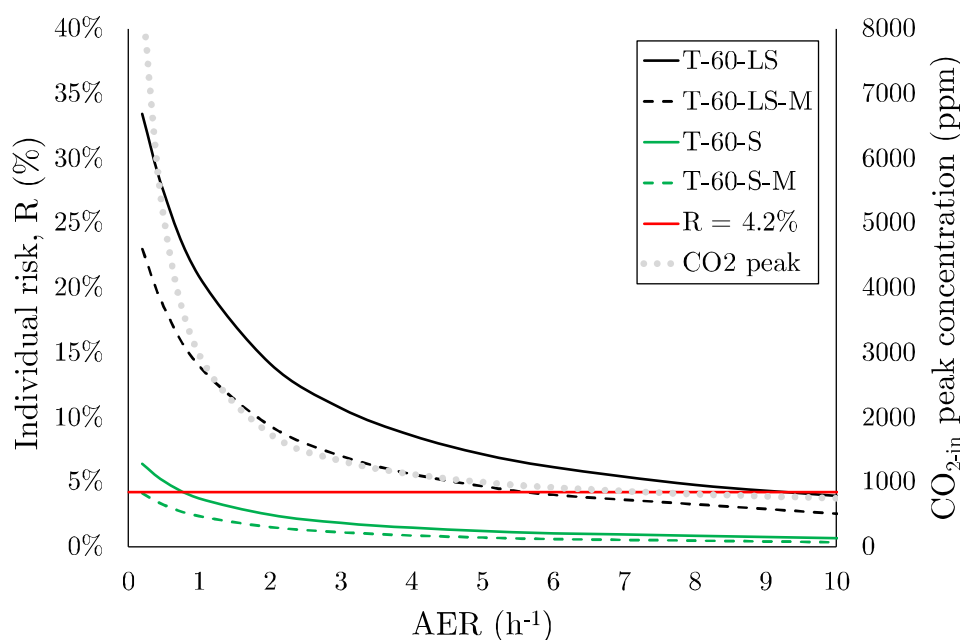
Table 3 – Required constant AER (h⁻¹) to maintain a $R_{event} < 1$ for all the scenarios investigated for SARS-CoV-2 for mechanically-ventilated classrooms.

Scenarios		AER (h ⁻¹)
Base scenarios	T-60-LS	9.5
	S-0%-S	0.8
Student's speaking effect	S-10%-S	1.5
	S-20%-S	2.1
	S-30%-S	2.8
	S-40%-S	3.5
	T-55-LS	8.6
Class duration effect	T-50-LS	7.8
	T-45-LS	6.9
	T-40-LS	6.1
	Voice modulation effect	T-60-S
Mask effect	T-60-LS-M	5.8
Voice modulation & mask effect	T-60-S-M	0.2

316
317
318

In Figure 2 the individual risk, R , of students for different exposure scenarios characterized by the presence of a SARS-CoV-2-infected teacher giving lesson for 60 min as a function of the air exchange

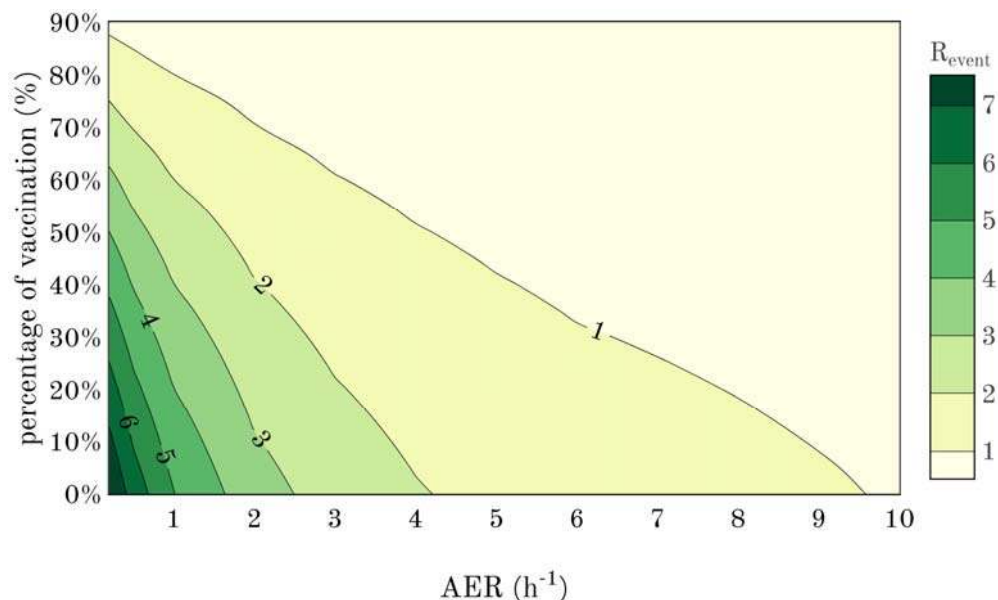
319 rate provided by a mechanical ventilation system is presented. In particular, the base scenario
 320 (teacher loudly speaking) and the mitigation solutions (voice modulation and use of mask) are
 321 graphed. As expected the individual risk clearly decreases for higher AERs and, as summarized in
 322 Table 3, very high AERs are required for the teacher when loudly speaking. Such high AERs are likely
 323 not reproducible in schools without mechanical ventilation systems; indeed, in our previous papers
 324 [31,56,58,60] we have estimated that the AER, when no airing procedures are imposed, are typically
 325 lower than 1 h^{-1} and that the AER for manual airing (mainly side-ventilation) are $< 5 \text{ h}^{-1}$. Figure 2
 326 presents the expected peak CO_2 concentrations (i.e. at the end of the school-day) as a function of the
 327 AERs and clearly shows that the CO_2 level per se could be extremely misleading when not interpreted
 328 with a specific focus on infection transmission. Indeed, even when acceptable CO_2 levels are provided
 329 (e.g. $< 1000 \text{ ppm}$), an unacceptable individual risk can occur. For high-emitting activities (i.e. loudly
 330 speaking) the mitigation solutions (e.g. the use of microphones) are more effective than the classroom
 331 ventilation itself. Furthermore, there is a transient aspect to the problem when CO_2 concentrations
 332 start at a low level and then build up to an established acceptable level, all the while inhalation of
 333 infectious particles (droplet nuclei) may be occurring.
 334



335
 336 **Figure 2** – Individual risk, R (%), of students for different exposure scenarios characterized by the presence of a
 337 SARS-CoV-2 infected teacher giving lesson for 60 min as a function of the air exchange rate for mechanically-
 338 ventilated classrooms: loudly speaking (T-60-LS), speaking (T-60-S), loudly speaking and wearing mask (T-60-
 339 LS-M), speaking and wearing mask (T-60-S-M). Expected CO_2 peak concentrations (i.e. at the end of the school-
 340 day) as a function of the AERs are also reported.

341 The high AERs required in some of the above-mentioned scenarios can be higher than those typically
 342 suggested by the current indoor air quality standards defined by the EN 15251 [48]. Indeed, the EN
 343 15251 provides the AERs as a function of the category of the indoor air quality (I, II, or III) and
 344 categories of pollution from building itself (very low polluting building, low polluting building, non low
 345 polluting building). As an example, for the classroom under investigation the air exchange rates
 346 suggested by the standard would be: 6.6 h^{-1} (very low polluting building), 7.2 h^{-1} (low polluting
 347 building) and 8.4 h^{-1} (non low polluting building) for building category I, 4.6 h^{-1} , 5.0 h^{-1} , and 5.9 h^{-1} , for
 348 building category II, and 2.6 h^{-1} , 2.9 h^{-1} , and 3.4 h^{-1} for building category III, respectively. Thus, for such
 349 a critical scenario, in order to maintain a $R_{\text{event}} < 1$ at lower air exchange rates the number of
 350 susceptibles (S) should be reduced; to this end the most effective solution is increasing the vaccination
 351 fraction of the population. As an example, in Figure 3 the R_{event} as a function of the air exchange rate
 352 (provided through a mechanical ventilation system) and of the percentage of vaccination for the T-60-
 353 LS scenario is reported. The figure clearly highlights that for such a critical scenario a percentage of
 354 vaccinated people $> 60\%$ (i.e. > 14 persons) would allow reducing the required air exchange rate to

355 about 3 h⁻¹, i.e. to the AER suggested by the EN 15251 for building category III which is, by the way, the
356 category recommended by the standard for existing buildings. The graph also confirms that reopening
357 naturally ventilated schools by allowing up to 50% attendance as adopted in several countries would
358 not guarantee a low transmission potential of the SARS-CoV-2, at least for highly emitting infected
359 subjects.
360



361
362 **Figure 3** – R_{event} for the T-60-LS scenario as a function of the air exchange rate (provided through a mechanical
363 ventilation system) and of the percentage of vaccination.

364 As mentioned in the methodology (section 2.4), for mechanically-ventilated classrooms, the $R_{event} < 1$
365 condition can be maintained if the required AERs obtained for the selected scenarios are adopted. In
366 particular, in that case, a simple constant air volume flow system is enough to provide the required
367 AER and no complex control algorithms, typical of demand-controlled ventilation systems, are needed.
368 In fact, once the scenario is defined, in principle no feedback information is required: a possible
369 procedure in the case of schools equipped with mechanical ventilation is schematically presented in
370 Figure 4. In particular, data regarding the expected scenario (e.g. teacher giving lesson for the first 60
371 min of the school-day using a microphone; total exposure time; classroom volume) should be provided
372 to the control unit (e.g. inputting through a user input screen) that will be able to evaluate the required
373 AER on the basis of the equations reported in the section 2.1 and, consequently, will set the needed air
374 flow rate of the mechanical ventilation system. In other words, different modes of operation can be
375 selected based on pre-determined activities and durations for the classroom (e.g. lecture, lunch,
376 exercise activity, etc.). Optimizing the provided ventilation based on demand is important given the
377 high energy cost of conditioning outside air in many climates [60–64]; however, our proposed strategy
378 for practical infection control is based on the activities of the occupants rather than CO₂ *a priori*.
379 Where activity schedules are consistent, modes of operation can be scheduled in advance to eliminate
380 the need for constant adjustment.

381 3.2 Airing procedures for naturally-ventilated schools

382 In the case of school without mechanical ventilation, maintaining a $R_{event} < 1$ is a challenge for
383 scenarios characterized by high emitting infected subjects for two main reasons: i) keeping the
384 windows opened could be not enough to guarantee very high fresh air flow rates, ii) keeping the
385 windows opened for long periods could be detrimental for thermal comfort and energy conservation
386 purposes [58,60,65]. Adopting manual airing cycles described in the section 2.4 represents a practical
387 solution, but it should be kept in mind that the scheduling of window opening and closing period can
388 affect the infection risk of the exposed susceptibles and a required AER cannot be determined *a-priori*.
389 As an example, if AER_{NV} and AER_{MA} were a constant 0.2 and 4.0 h⁻¹, respectively, for the scenario T-60-

390 S, a $R_{\text{event}} < 1$ (i.e. $R = 4.2\%$) could be obtained opening the windows for about 10 min at the end of
391 each hour. The resulting school-day average AER would be equal to of 0.8 h^{-1} , which similar to that
392 needed in case of constant mechanical ventilation systems. But, for lower AERs, e.g. constant AER_{NV}
393 and AER_{MA} equal to 0.15 and 2.0 h^{-1} , respectively, the required opening period at the end of each hour
394 is 36 min then resulting in a school-day average AER of 1.3 h^{-1} which is significantly higher than that
395 required in the case of steady state mechanical ventilation system. These two easy examples, highlight
396 that the lower the AER_{NV} and AER_{MA} values, the longer the required airing period and, consequently,
397 the higher the resulting school-day average AER.

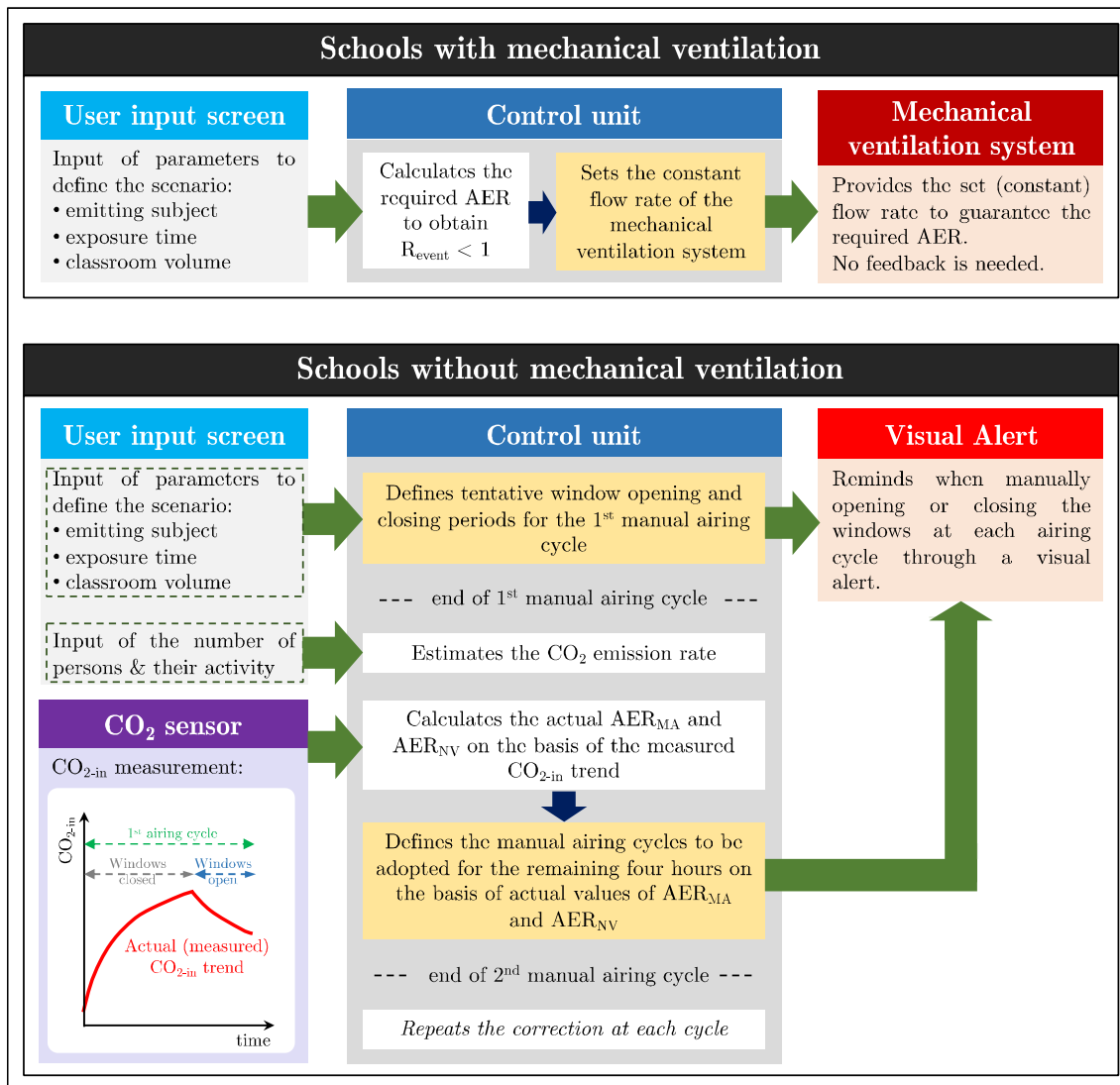
398 Thus, the airing strategies are strongly affected by the air exchange rate values, therefore adopting
399 scheduled airing procedures could be misleading. In October 2020 the German Environment Agency
400 (UBA) issued guidance for schools recommending airing classrooms for 5 minutes after every 20
401 minutes (www.umweltbundesamt.de/en/press/pressinformation/coronavirus-protection-in-schools-airing-rooms-for). For the T-60-S scenario, in the likely hypothesis of having AER_{NV} at least equal to
402 0.2 h^{-1} , adopting the German procedure would allow maintaining a $R_{\text{event}} < 1$ only for $AER_{\text{MA}} > 3.3 \text{ h}^{-1}$;
403 however, such an air exchange rate during manual airing could be not reached.

404 The above-mentioned examples highlight how AER_{NV} and AER_{MA} need to be continuously monitored so
405 that the airing procedure can be adjusted in real-time. This procedure is obviously more complex than
406 providing mechanical ventilation, and the support of control unit is even more important as it should
407 be able to communicate with a CO_2 sensor and provide visual alerts on when opening and closing the
408 windows, which will be performed manually by personnel in the classroom (e.g. teacher).

409 Alternatively, since it may be challenging to have a teacher or student reliably open and close a
410 window in response to frequent prompts from the control unit, for relatively minor incremental cost
411 one or more windows in the room could be fitted with a motorized louver, or damper, connected to
412 the control unit such that the percent open of the window can be automatically adjusted by the system.

413 Anyway, whatever the windows are automatically or manually opened, the ventilation procedure is
414 equivalent and provided by the control unit. Indeed, data regarding the expected scenario will be
415 provided to the control unit (through the user input screen as well), then the control unit will evaluate
416 and suggest the manual airing procedure to be adopted in order to guarantee a $R_{\text{event}} < 1$. In particular,
417 the control unit will use as feedback information the indoor CO_2 concentration continuously measured
418 by an in-room sensor and, on the basis of the number of persons and their activity levels (that will be
419 provided through the user input screen) and of the initial indoor CO_2 concentration, it will back-
420 calculate the actual AERs during both the period with windows close (AER_{NV}) and open (AER_{MA}) using
421 the CO_2 mass balance equation (eq. 7) (Figure 4). Such calculation should be performed adopting a
422 multi-points method, i.e. finding the best regression fit to the continuous CO_2 data, which is more
423 accurate than the two-points method (i.e. considering just the CO_2 measurement of start point and end
424 point of natural ventilation and manual airing periods) [66] since it will be less affected by CO_2 sensor
425 accuracy and intermittent "noisy" measurements. On the basis of the actual AERs the corrected t_{MA} and
426 t_{NV} periods will be calculated by the control unit and the windows opening periods will be scheduled
427 as well for the further four hours (i.e. four cycles) in order to obtain a $R_{\text{event}} < 1$. Since the AER_{NV} and
428 AER_{MA} values are not known *a-priori*, during the first hour/cycle tentative opening and closing periods
429 can be adopted (e.g. 50 min with windows closed and 10 min with windows open). Then, the
430 measurement of the actual AERs will allow scheduling the equally-spaced opening periods of the
431 remaining four hours in order to obtain a $R_{\text{event}} < 1$ (i.e. $R = 4.2\%$) including the entire school-day (i.e.
432 five hours) in the calculation. The scheduled opening and closing periods also consider that if the
433 infected teacher gives lesson on the second, third, fourth or fifth hour the $R_{\text{event}} < 1$ condition must be
434 verified. Actually, the latest the infected teacher enters the classroom, the shorter the exposure period
435 of the susceptible persons (students in this case), this is the reason why we have considered the first
436 hour in the simulations as worst scenario. Counterintuitively, for very different airing periods amongst
437 the airing cycles, the resulting risk for exposed people could be higher for teacher entering the
438 classroom on the last hours than on the first ones, illustrating the need for real-time feedback on what
439 is going on in the classroom. This could be partially solved scheduling equally-spaced opening periods
440 as mentioned above; nonetheless, the control unit needs to check if the opening periods based on
441 actual AERs can guarantee a $R_{\text{event}} < 1$ also for infected teacher entering the classroom at different
442 hours.
443

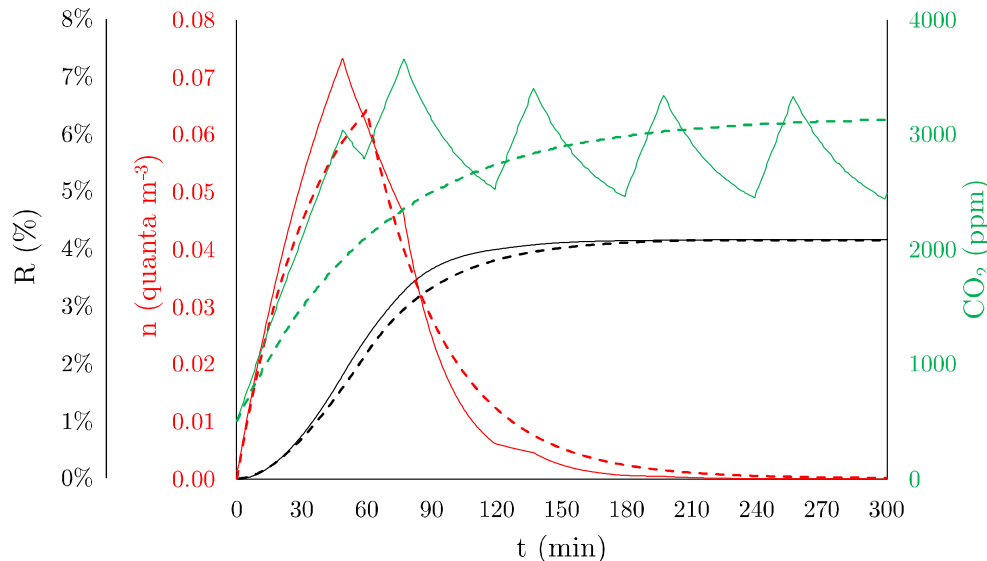
444 At the end of the second cycle AER_{NV} and AER_{MA} will be back-calculated again and, in case, the opening
 445 and closing periods will be modified again. Indeed, a high variability of the air exchange rate with
 446 windows open could occur, thus, significant corrections may be needed.
 447



448 **Figure 4** – Scheme of the suggested procedures to be applied in schools with and without mechanical ventilation
 449 to maintain $R_{event} < 1$.
 450

451 An example application of the correction procedure is presented in Figure 5 for the scenario T-60-S. In
 452 the figure the indoor CO_2 concentration, SARS-CoV-2 quanta concentration, and individual risk trend
 453 are presented. During the first hour a tentative airing cycle made up of 50 min with windows closed
 454 and 10 min with windows open was adopted. From the CO_2 trend, the actual AER_{NV} and AER_{MA} values
 455 were back-calculated and (in this illustrative example) are equal to 0.15 and 2.0 h^{-1} , respectively. On
 456 the basis of the actual AERs, in order to maintain a $R_{event} < 1$ (i.e. $R = 4.2\%$), the control unit schedules
 457 equally-spaced window opening periods of 42 min for the remaining four hours to be applied at the
 458 end of each hour. Thus, the total times during which the windows were kept closed and open for the
 459 entire school day are $t_{NV} = 122$ min and $t_{MA} = 178$ min (having included the 50 min and 10 min of
 460 window closing and opening periods of the first hour) then resulting in a school-day average AER of
 461 about 1.3 h^{-1} . The tentative opening and closing periods adopted for the first hour were then too short
 462 compared to the actual low AERs, for this reason the quanta concentration in the first hour increases
 463 significantly and the individual risk trend as well with respect to the same scenario occurring in a
 464 classroom equipped with a mechanical ventilation system where a constant $AER = 0.8 \text{ h}^{-1}$ is enough to

465 maintain $R_{event} < 1$. The scheduled opening and closing periods also maintain a $R_{event} < 1$ if the infected
 466 teacher gave lesson in the second ($R = 4.1\%$), third ($R = 4.1\%$), fourth ($R = 3.8\%$) or fifth hour
 467 ($R = 2.4\%$). In this example the actual AERs were considered constant during the entire school-day,
 468 nonetheless, if the AERs at the end of each closing and opening periods do not match with the expected
 469 ones (0.15 and 2.0 h^{-1} in this example) further corrections are needed at the end of each hour.
 470



471
 472 **Figure 5** – Trends of quanta concentration (n), individual risk (R), and indoor CO_2 concentration (CO_{2-in}) for the
 473 scenario T-60-S in the case of SARS-CoV-2 to maintain a $R_{event} < 1$ through (a) mechanical ventilation system
 474 (constant AER = 0.8 h^{-1} ; bold dotted lines) and (b) manual airing procedures corrected for actual AER (school-
 475 day average AER = 1.3 h^{-1} in the hypothesis of measured AER_{NV} and AER_{MA} of 0.15 and 2.0 h^{-1} , respectively; thin
 476 solid lines).

477 3.3 Applicability and limitation of the methodology for ventilation control

478 The methodology presented in the paper addresses the proposed goals of (i) quantifying the required
 479 ventilation (provided through mechanical systems or manual airing) to reduce the spread of infectious
 480 diseases via the airborne route and (ii) proposing a suitable feedback control strategy to monitor and
 481 adjust such ventilation in naturally-ventilated classrooms. Nonetheless, in order to effectively reduce
 482 the transmission potential of a disease, the uncertainty of the event reproduction number (R_{event})
 483 should be taken into account such that, the required air exchange rate maintains $(R_{event} - U_{Revent}) < 1$,
 484 with U_{Revent} representing the expanded uncertainty (e.g. with a coverage factor of 95%). The evaluation
 485 of U_{Revent} cannot be easily evaluated as it depends on several parameters and models adopted in the
 486 calculations presented in the section 2.1 (eq. 1-5). Indeed, when evaluating the R_{event} (eq. 1-5) the
 487 following data are needed: quanta emission rate (ER_q), deposition rate (k), inactivation rate (λ),
 488 inhalation rate (IR), room volume (V), air exchange rate (AER), time of exposure (T). The quanta
 489 emission rate was investigated in our previous papers where we highlighted that uncertainty relates
 490 to the quality of data on viral load, infectious dose and particle volume: such data, at least for SARS-
 491 CoV-2, are not definitive [44,51,67] also due to the presence of different viral lineages [68]. Therefore,
 492 even if the ER_q data provided by our model are much more suitable than those typically estimated
 493 based on retrospective assessments of infectious outbreaks, a not negligible uncertainty exists. The
 494 deposition rate is mainly affected by the particle size [55] and, thus, adopting an average parameter, as
 495 typical of easy-to-use box-models, results in additional uncertainty as well; similarly, data on the virus
 496 inactivation rate for SARS-CoV-2 are still limited [53,69]. The inhalation rate depends on the activity
 497 levels of the subject; different scientific papers [42,70] reported different IR values for the same
 498 activity then confirming a significant variability as well. Room volume and time of exposure can be
 499 considered as fixed values (or at least with a not significant uncertainty contribution) as well as the
 500 AER if provided through a mechanical ventilation system. The uncertainty budget should also include

501 the physical limitations of the box model (i.e. homogeneous concentration within the room), particle
502 dosimetry model, and dose-response model as well.
503 The uncertainty budget would be even more complex for confined spaces without mechanical
504 ventilation where manual airing procedures, corrected on the basis of the measured CO₂ values, are
505 put in place. Indeed, in this case, the uncertainty of the CO₂ measurements and of the CO₂ mass balance
506 equation (“constant injection rate method” [32,47]) to back-calculate the corrected AERs should be
507 included too. The effect of the CO₂ measurement uncertainty is quite straightforward: indeed, in view
508 of correcting the manual airing cycles on the basis of the CO₂ measurement, a higher CO₂ uncertainty
509 would undermine the back-calculation of the actual AERs. The CO₂ measurement uncertainty is
510 typically affected by the sensor accuracy, resolution, temperature effect, static pressure effect, dew-
511 point effect, and probe positioning within the room [71]. CO₂ probes should be able to provide
512 measurement data with an expanded accuracy of about 5% [71,72], but low-cost sensors may presents
513 larger uncertainties. Nonetheless, as mentioned above, adopting a multi-points method could
514 overcome the problem of the CO₂ sensor accuracy [66] and significantly reduce the AER uncertainty
515 contribution with respect to two-point method. Indeed, the CO₂ measurement uncertainty could
516 represent a secondary contribution to the AER back-calculation through the eq. 7, in fact, the
517 uncertainty of the exhaled CO₂ emission rate could mainly affect the AER uncertainties [73,74].
518 Summarizing, the uncertainty budget of R_{event} is quite complex and beyond the aims of the current
519 paper. Further studies, in particular those applying real-world measurements and data, are needed in
520 view of improving the quantification of the virus transmission potential for different ventilation
521 systems.

522 4 Conclusions

523 The study provides a method to support regulatory authorities in the safe operation of schools in the
524 time of pandemics. To this end the required ventilation to reduce the spread of infectious diseases via
525 the airborne route was assessed for both mechanically-and naturally-ventilated classrooms through
526 virus mass balance equations. For the latter, which represent the more frequent and also the more
527 challenging situation, a suitable feedback control strategy based on exhaled CO₂ monitoring was also
528 proposed in view of maintaining a limited transmission potential of the disease.
529 The scenarios simulated revealed that adopting a CO₂ concentration threshold as a possible proxy for
530 virus transmission can be misrepresentative. Indeed, the dynamics of the virus-laden particles and the
531 occurrence of the virus emission may strongly differ from the exhaled CO₂ ones, thus, CO₂ and virus
532 concentrations (expressed as “quanta” concentrations) may present significantly different trends.
533 Seasonal influenza presents a negligible transmission potential via airborne route in classroom, even
534 when low ventilation is provided; this is due to the low emission rates typical of such virus. On the
535 contrary, the required air exchange rates to guarantee a $R_{event} < 1$ for SARS-CoV-2 can be very high for
536 scenarios characterized by highly-emitting infected subjects, such as teacher loudly speaking. Such
537 AERs could be even higher than those suggested by the indoor air quality technical standards, thus,
538 mitigation solutions (e.g. voice modulation in particular) or adequate immunization coverage (i.e. high
539 vaccination percentage) are welcomed.
540 In order to reduce the virus transmission potential, *ad-hoc* procedures were defined in the case of both
541 mechanically- and naturally-ventilated classrooms. For mechanically-ventilated classrooms a very
542 straightforward procedure was defined since, once the scenario (in terms of emitting subject,
543 classroom geometry, etc.), a control unit can calculate the required air exchange rate accordingly and
544 set the corresponding constant fresh flow rate of the mechanical ventilation system. Such a scenario
545 can be established as a selectable mode of operation for the control unit.
546 For naturally-ventilated classrooms a suitable feedback control strategy was included and applied in
547 the method. In these classrooms, manual airing cycles help increase the air exchange rate but, due to
548 the dynamic of the emission and of the airing cycles, a required air exchange rate cannot be defined *a-*
549 *priori*. Thus, the design parameter is not just the air exchange rate but the $R_{event} < 1$ condition itself
550 which informs scheduling of the manual airing procedures. Such manual airing would be continuously
551 checked and, in case, re-scheduled on the basis of the indoor CO₂ concentration monitoring. The
552 monitoring would allow evaluation of the actual ventilation rates during the airing cycles and inform
553 proper adjustments to the airing periods.

554 While further efforts are needed to quantify and reduce the uncertainties of the models, parameters
555 and measured data in the evaluation of individual risk and virus transmission potential, the suggested
556 method provide critical support for national public health authorities to minimize the contribution of
557 school environments to the spread of the pandemics.
558
559

560 **References**

- 561 [1] S. Chang, E. Pierson, P.W. Koh, J. Gerardin, B. Redbird, D. Grusky, J. Leskovec, Mobility network
562 models of COVID-19 explain inequities and inform reopening, *Nature*. 589 (2021) 82–87.
563 <https://doi.org/10.1038/s41586-020-2923-3>.
- 564 [2] S.L. Miller, W.W. Nazaroff, J.L. Jimenez, A. Boerstra, G. Buonanno, S.J. Dancer, J. Kurnitski, L.C.
565 Marr, L. Morawska, C. Noakes, Transmission of SARS-CoV-2 by inhalation of respiratory aerosol in the
566 Skagit Valley Chorale superspreading event, *Indoor Air*. n/a (2020).
567 <https://doi.org/10.1111/ina.12751>.
- 568 [3] L. Morawska, J.W. Tang, W. Bahnfleth, P.M. Bluyssen, A. Boerstra, G. Buonanno, J. Cao, S. Dancer,
569 A. Floto, F. Franchimon, C. Haworth, J. Hogeling, C. Isaxon, J.L. Jimenez, J. Kurnitski, Y. Li, M. Loomans, G.
570 Marks, L.C. Marr, L. Mazzarella, A.K. Melikov, S. Miller, D.K. Milton, W. Nazaroff, P.V. Nielsen, C. Noakes,
571 J. Peccia, X. Querol, C. Sekhar, O. Seppänen, S. Tanabe, R. Tellier, K.W. Tham, P. Wargocki, A. Wierzbicka,
572 M. Yao, How can airborne transmission of COVID-19 indoors be minimised?, *Environment*
573 *International*. 142 (2020) 105832. <https://doi.org/10.1016/j.envint.2020.105832>.
- 574 [4] B. Blocken, T. van Druenen, T. van Hooff, P.A. Verstappen, T. Marchal, L.C. Marr, Can indoor
575 sports centers be allowed to re-open during the COVID-19 pandemic based on a certificate of
576 equivalence?, *Building and Environment*. 180 (2020) 107022.
577 <https://doi.org/10.1016/j.buildenv.2020.107022>.
- 578 [5] G. Buonanno, L. Morawska, L. Stabile, Quantitative assessment of the risk of airborne
579 transmission of SARS-CoV-2 infection: Prospective and retrospective applications, *Environment*
580 *International*. 145 (2020) 106112. <https://doi.org/10.1016/j.envint.2020.106112>.
- 581 [6] G. Buonanno, L. Stabile, L. Morawska, Estimation of airborne viral emission: Quanta emission
582 rate of SARS-CoV-2 for infection risk assessment, *Environment International*. 141 (2020) 105794.
583 <https://doi.org/10.1016/j.envint.2020.105794>.
- 584 [7] T.P. Baggett, H. Keyes, N. Sporn, J.M. Gaeta, Prevalence of SARS-CoV-2 Infection in Residents of
585 a Large Homeless Shelter in Boston, *JAMA*. 323 (2020) 2191–2192.
586 <https://doi.org/10.1001/jama.2020.6887>.
- 587 [8] Y. Li, G.M. Leung, J.W. Tang, X. Yang, C.Y.H. Chao, J.Z. Lin, J.W. Lu, P.V. Nielsen, J. Niu, H. Qian, A.C.
588 Sleigh, H.-J.J. Su, J. Sundell, T.W. Wong, P.L. Yuen, Role of ventilation in airborne transmission of
589 infectious agents in the built environment - a multidisciplinary systematic review., *Indoor Air*. 17
590 (2007) 2–18. <https://doi.org/10.1111/j.1600-0668.2006.00445.x>.
- 591 [9] R.M. Viner, S.J. Russell, H. Croker, J. Packer, J. Ward, C. Stansfield, O. Mytton, C. Bonell, R. Booy,
592 School closure and management practices during coronavirus outbreaks including COVID-19: a rapid
593 systematic review, *School Closure and Management Practices during Coronavirus Outbreaks Including*
594 *COVID-19: A Rapid Systematic Review*. (2020). [https://doi.org/10.1016/s2352-4642\(20\)30095-x](https://doi.org/10.1016/s2352-4642(20)30095-x).
- 595 [10] M. Klimek-Tulwin, T. Tulwin, Early school closures can reduce the first-wave of the COVID-19
596 pandemic development, *Journal of Public Health*. (2020). <https://doi.org/10.1007/s10389-020-01391-z>.
- 598 [11] J. Bayham, E.P. Fenichel, Impact of school closures for COVID-19 on the US health-care
599 workforce and net mortality: a modelling study, *The Lancet Public Health*. 5 (2020) e271–e278.
600 [https://doi.org/10.1016/S2468-2667\(20\)30082-7](https://doi.org/10.1016/S2468-2667(20)30082-7).
- 601 [12] J. Zhang, Y. Hayashi, L.D. Frank, COVID-19 and transport: Findings from a world-wide expert
602 survey, *Transport Policy*. 103 (2021) 68–85. <https://doi.org/10.1016/j.tranpol.2021.01.011>.
- 603 [13] K. Farsalinos, K. Poulas, D. Kouretas, A. Vantarakis, M. Leotsinidis, D. Kouvelas, A.O. Docea, R.
604 Kostoff, G.T. Gerotziakas, M.N. Antoniou, R. Polosa, A. Barbouni, V. Yiakoumaki, T.V. Giannouchos, P.G.
605 Bagos, G. Lazopoulos, B.N. Izotov, V.A. Tutelyan, M. Aschner, T. Hartung, H.M. Wallace, F. Carvalho, J.L.
606 Domingo, A. Tsatsakis, Improved strategies to counter the COVID-19 pandemic: Lockdowns vs.
607 primary and community healthcare, *Toxicology Reports*. 8 (2021) 1–9.
608 <https://doi.org/10.1016/j.toxrep.2020.12.001>.

- 609 [14] D.R. Petretto, I. Masala, C. Masala, School Closure and Children in the Outbreak of COVID-19,
610 Clin Pract Epidemiol Ment Health. 16 (2020) 189–191.
611 <https://doi.org/10.2174/1745017902016010189>.
- 612 [15] W. Chen, N. Zhang, J. Wei, H.-L. Yen, Y. Li, Short-range airborne route dominates exposure of
613 respiratory infection during close contact, Building and Environment. 176 (2020) 106859.
614 <https://doi.org/10.1016/j.buildenv.2020.106859>.
- 615 [16] Z.T. Ai, A.K. Melikov, Airborne spread of expiratory droplet nuclei between the occupants of
616 indoor environments: A review., Indoor Air. 28 (2018) 500–524. <https://doi.org/10.1111/ina.12465>.
- 617 [17] Z.T. Ai, K. Hashimoto, A.K. Melikov, Airborne transmission between room occupants during
618 short-term events: Measurement and evaluation, Indoor Air. 29 (2019) 563–576.
619 <https://doi.org/10.1111/ina.12557>.
- 620 [18] W.J. Edmunds, Finding a path to reopen schools during the COVID-19 pandemic, The Lancet
621 Child & Adolescent Health. 4 (2020) 796–797. [https://doi.org/10.1016/S2352-4642\(20\)30249-2](https://doi.org/10.1016/S2352-4642(20)30249-2).
- 622 [19] N. Ziauddeen, K. Woods-Townsend, S. Saxena, R. Gilbert, N.A. Alwan, Schools and COVID-19:
623 Reopening Pandora’s box?, Public Health in Practice. 1 (2020) 100039.
624 <https://doi.org/10.1016/j.puhip.2020.100039>.
- 625 [20] N.H.L. Leung, D.K.W. Chu, E.Y.C. Shiu, K.-H. Chan, J.J. McDevitt, B.J.P. Hau, H.-L. Yen, Y. Li, D.K.M.
626 Ip, J.S.M. Peiris, W.-H. Seto, G.M. Leung, D.K. Milton, B.J. Cowling, Respiratory virus shedding in exhaled
627 breath and efficacy of face masks, Nature Medicine. 26 (2020) 676–680.
628 <https://doi.org/10.1038/s41591-020-0843-2>.
- 629 [21] L. Morawska, J. Cao, Airborne transmission of SARS-CoV-2: The world should face the reality,
630 Environment International. 139 (2020) 105730. <https://doi.org/10.1016/j.envint.2020.105730>.
- 631 [22] R. Tellier, Aerosol transmission of influenza A virus: a review of new studies., J R Soc Interface.
632 6 Suppl 6 (2009) S783–790. <https://doi.org/10.1098/rsif.2009.0302.focus>.
- 633 [23] S. Tang, Y. Mao, R.M. Jones, Q. Tan, J.S. Ji, N. Li, J. Shen, Y. Lv, L. Pan, P. Ding, X. Wang, Y. Wang,
634 C.R. MacIntyre, X. Shi, Aerosol transmission of SARS-CoV-2? Evidence, prevention and control, Environ
635 Int. 144 (2020) 106039–106039. <https://doi.org/10.1016/j.envint.2020.106039>.
- 636 [24] S.N. Rudnick, D.K. Milton, Risk of indoor airborne infection transmission estimated from carbon
637 dioxide concentration., Indoor Air. 13 (2003) 237–245. <https://doi.org/10.1034/j.1600-0668.2003.00189.x>.
- 639 [25] P. de Man, S. Paltansing, D.S.Y. Ong, N. Vaessen, G. van Nielen, J.G.M. Koeleman, Outbreak of
640 Coronavirus Disease 2019 (COVID-19) in a Nursing Home Associated With Aerosol Transmission as a
641 Result of Inadequate Ventilation, Clinical Infectious Diseases. (2020).
642 <https://doi.org/10.1093/cid/ciaa1270>.
- 643 [26] R.M. Baloch, C.N. Maesano, J. Christoffersen, S. Banerjee, M. Gabriel, É. Csobod, E. de Oliveira
644 Fernandes, I. Annesi-Maesano, É. Csobod, P. Szuppinger, R. Prokai, P. Farkas, C. Fuzi, E. Cani, J.
645 Draganic, E.R. Mogyorosy, Z. Korac, E. de Oliveira Fernandes, G. Ventura, J. Madureira, I. Paciência, A.
646 Martins, R. Pereira, E. Ramos, P. Rudnai, A. Páldy, G. Dura, T. Beregszászi, É. Vaskövi, D. Magyar, T.
647 Pándics, Z. Remény-Nagy, R. Szentmihályi, O. Udvardy, M.J. Varró, S. Kephelopoulos, D. Kotzias, J.
648 Barrero-Moreno, R. Mehmeti, A. Vilic, D. Maestro, H. Moshammer, G. Strasser, P. Brigitte, P.
649 Hohenblum, E. Goelen, M. Stranger, M. Spruy, M. Sidjimov, A. Hadjipanayis, A. Katsonouri-Sazeides, E.
650 Demetriou, R. Kubinova, H. Kazmarová, B. Dlouha, B. Kotlík, H. Vabar, J. Ruut, M. Metus, K. Rand, A.
651 Järviste, A. Nevalainen, A. Hyvarinen, M. Täubel, K. Järvi, I. Annesi-Maesano, C. Mandin, B. Berthineau,
652 H.-J. Moriske, M. Giacomini, A. Neumann, J. Bartzis, K. Kalimeri, D. Saraga, M. Santamouris, M.N.
653 Assimakopoulos, V. Asimakopoulos, P. Carrer, A. Cattaneo, S. Pulvirenti, F. Vercelli, F. Strangi, E. Omeri,
654 S. Piazza, A. D’Alcamo, A.C. Fanetti, P. Sestini, M. Kouri, G. Viegi, G. Sarno, S. Baldacci, S. Maio, S. Cerrai,
655 V. Franzitta, S. Bucchieri, F. Cibella, M. Simoni, M. Neri, D. Martuzevičius, E. Krugly, S. Montefort, P.
656 Fsadni, P.Z. Brewczykński, E. Krakowiak, J. Kurek, E. Kubarek, A. Wlazło, C. Borrego, C. Alves, J. Valente,
657 E. Gurzau, C. Rosu, G. Popita, I. Neamtii, C. Neagu, D. Norback, P. Bluyssen, M. Bohms, P. Van Den Hazel,

- 658 F. Cassee, Y.B. de Bruin, A. Bartonova, A. Yang, K. Halzlová, M. Jajcaj, M. Kániková, O. Miklankova, M.
659 Vítkivá, M. Jovsevic-Stojanovic, M. Zivkovic, Z. Stevanovic, I. Lazovic, Z. Stevanovic, Z. Zivkovic, S.
660 Cerovic, J. Jovic-Stojanovic, D. Mumovic, P. Tarttelin, L. Chatzidiakou, E. Chatzidiakou, M.-C. Dewolf,
661 Indoor air pollution, physical and comfort parameters related to schoolchildren's health: Data from the
662 European SINPHONIE study, *Science of The Total Environment*. 739 (2020) 139870.
663 <https://doi.org/10.1016/j.scitotenv.2020.139870>.
- 664 [27] E. Csobod Annesi-Maesano, I., Carrer, P., Kephelopoulos, S., Madureira, J., Rudnai, P., De
665 Oliveira Fernandes, E., Barrero, J., Beregszászi, T., Hyvärinen, A., Moshammer, H., Norback, D., Páldy,
666 A., Pándics, T., Sestini, P., Stranger, M., Taubel, M., Varró, M., Vaskovi, E., Ventura Silva, G. Vieg, G.,,
667 SINPHONIE – Schools Indoor Pollution and Health Observatory Network in Europe - Final Report,
668 Publications Office of the European Union, Luxembourg, 2014.
- 669 [28] S. Zhu, S. Jenkins, K. Addo, M. Heidarinejad, S.A. Romo, A. Layne, J. Ehizibolo, D. Dalgo, N.W.
670 Mattise, F. Hong, O.O. Adenaiye, J.P. Bueno de Mesquita, B.J. Albert, R. Washington-Lewis, J. German, S.
671 Tai, S. Youssefi, D.K. Milton, J. Srebric, Ventilation and laboratory confirmed acute respiratory infection
672 (ARI) rates in college residence halls in College Park, Maryland, *Environment International*. 137
673 (2020) 105537. <https://doi.org/10.1016/j.envint.2020.105537>.
- 674 [29] B. Pavilonis, A.M. Ierardi, L. Levine, F. Mirer, E.A. Kelvin, Estimating Aerosol Transmission Risk
675 of SARS-CoV-2 in New York City Public Schools During Reopening, *Environ Res.* (2021) 110805–
676 110805. <https://doi.org/10.1016/j.envres.2021.110805>.
- 677 [30] A. Pacitto, L. Stabile, L. Morawska, M. Nyarku, M.A. Torkmahalleh, Z. Akhmetvaliyeva, A.
678 Andrade, F.H. Dominski, P. Mantecca, W.H. Shetaya, M. Mazaheri, R. Jayaratne, S. Marchetti, S.K. Hassan,
679 A. El-Mekawy, E.F. Mohamed, L. Canale, A. Frattolillo, G. Buonanno, Daily submicron particle doses
680 received by populations living in different low- and middle-income countries, *Environmental*
681 *Pollution*. 269 (2021) 116229. <https://doi.org/10.1016/j.envpol.2020.116229>.
- 682 [31] L. Stabile, G. Buonanno, A. Frattolillo, M. Dell'Isola, The effect of the ventilation retrofit in a
683 school on CO₂, airborne particles, and energy consumptions, *Building and Environment*. 156 (2019)
684 1–11. <https://doi.org/10.1016/j.buildenv.2019.04.001>.
- 685 [32] N. Mahyuddin, H.B. Awbi, A Review of CO₂ Measurement Procedures in Ventilation Research,
686 *International Journal of Ventilation*. 10 (2012) 353–370. [https://doi.org/10.5555/2044-4044-](https://doi.org/10.5555/2044-4044-10.4.353)
687 [10.4.353](https://doi.org/10.5555/2044-4044-10.4.353).
- 688 [33] Z. Bakó-Biró, D.J. Clements-Croome, N. Kochhar, H.B. Awbi, M.J. Williams, Ventilation rates in
689 schools and pupils' performance, *Building and Environment*. 48 (2) 215–223.
690 <https://doi.org/10.1016/j.buildenv.2011.08.018>.
- 691 [34] M.J. Mendell, E.A. Eliseeva, M.M. Davies, M. Spears, A. Lobscheid, W.J. Fisk, M.G. Apte,
692 Association of classroom ventilation with reduced illness absence: a prospective study in California
693 elementary schools., *Indoor Air*. 23 (2013) 515–528. <https://doi.org/10.1111/ina.12042>.
- 694 [35] C. Zemouri, S.F. Awad, C.M.C. Volgenant, W. Crielaard, A.M.G.A. Laheij, J.J. de Soet, Modeling of
695 the Transmission of Coronaviruses, Measles Virus, Influenza Virus, Mycobacterium tuberculosis, and
696 Legionella pneumophila in Dental Clinics., *J Dent Res*. 99 (2020) 1192–1198.
697 <https://doi.org/10.1177/0022034520940288>.
- 698 [36] R.K. Bhagat, M.S. Davies Wykes, S.B. Dalziel, P.F. Linden, Effects of ventilation on the indoor
699 spread of COVID-19, *Journal of Fluid Mechanics*. 903 (2020) F1.
700 <https://doi.org/10.1017/jfm.2020.720>.
- 701 [37] S.-Y. Cheng, C.J. Wang, A.C.-T. Shen, S.-C. Chang, How to Safely Reopen Colleges and Universities
702 During COVID-19: Experiences From Taiwan, *Ann Intern Med*. 173 (2020) 638–641.
703 <https://doi.org/10.7326/M20-2927>.
- 704 [38] A. Mikszewski, L. Stabile, G. Buonanno, L. Morawska, THE AIRBORNE CONTAGIOUSNESS OF
705 RESPIRATORY VIRUSES: A COMPARATIVE ANALYSIS AND IMPLICATIONS FOR MITIGATION,
706 *MedRxiv*. (2021) 2021.01.26.21250580. <https://doi.org/10.1101/2021.01.26.21250580>.

- 707 [39] P. Tupper, H. Boury, M. Yerlanov, C. Colijn, Event-specific interventions to minimize COVID-19
708 transmission, *Proc Natl Acad Sci USA*. 117 (2020) 32038. <https://doi.org/10.1073/pnas.2019324117>.
- 709 [40] T. Moreno, R.M. Pintó, A. Bosch, N. Moreno, A. Alastuey, M.C. Minguillón, E. Anfruns-Estrada, S.
710 Guix, C. Fuentes, G. Buonanno, L. Stabile, L. Morawska, X. Querol, Tracing surface and airborne SARS-
711 CoV-2 RNA inside public buses and subway trains, *Environment International*. 147 (2021) 106326.
712 <https://doi.org/10.1016/j.envint.2020.106326>.
- 713 [41] B.G. Wagner, B.J. Coburn, S. Blower, Calculating the potential for within-flight transmission of
714 influenza A (H1N1), *BMC Medicine*. 7 (2009) 81. <https://doi.org/10.1186/1741-7015-7-81>.
- 715 [42] W.C. Adams, Measurement of Breathing Rate and Volume in Routinely Performed Daily
716 Activities. Final Report. Human Performance Laboratory, Physical Education Department, University
717 of California, Davis., Human Performance Laboratory, Physical Education Department, University of
718 California, Davis. Prepared for the California Air Resources Board, Contract No. A033-205, April 1993.,
719 1993.
- 720 [43] International Commission on Radiological Protection, Human respiratory tract model for
721 radiological protection. A report of a Task Group of the International Commission on Radiological
722 Protection., *Annals of the ICRP*. 24 (1994) 1–482. [https://doi.org/10.1016/0146-6453\(94\)90029-9](https://doi.org/10.1016/0146-6453(94)90029-9).
- 723 [44] T. Watanabe, T.A. Bartrand, M.H. Weir, T. Omura, C.N. Haas, Development of a dose-response
724 model for SARS coronavirus., *Risk Anal*. 30 (2010) 1129–1138. <https://doi.org/10.1111/j.1539-6924.2010.01427.x>.
- 726 [45] G.N. Sze To, C.Y.H. Chao, Review and comparison between the Wells–Riley and dose-response
727 approaches to risk assessment of infectious respiratory diseases, *Indoor Air*. 20 (2010) 2–16.
728 <https://doi.org/10.1111/j.1600-0668.2009.00621.x>.
- 729 [46] A. Persily, L. de Jonge, Carbon dioxide generation rates for building occupants, *Indoor Air*. 27
730 (2017) 868–879. <https://doi.org/10.1111/ina.12383>.
- 731 [47] W.W. Nazaroff, Residential air-change rates: A critical review, *Indoor Air*. n/a (2021).
732 <https://doi.org/10.1111/ina.12785>.
- 733 [48] European Committee for Standardisation, UNI EN 15251 - Indoor environmental input
734 parameters for design and assessment of energy performance of buildings addressing indoor air
735 quality, thermal environment, lighting and acoustics, (2008).
- 736 [49] R.H. Alford, J.A. Kasel, P.J. Gerone, V. Knight, Human influenza resulting from aerosol
737 inhalation., *Proc Soc Exp Biol Med*. 122 (1966) 800–804. <https://doi.org/10.3181/00379727-122-31255>.
- 739 [50] P.J. Bueno de Mesquita, C.J. Noakes, D.K. Milton, Quantitative aerobiologic analysis of an
740 influenza human challenge-transmission trial, *Indoor Air*. 30 (2020) 1189–1198.
741 <https://doi.org/10.1111/ina.12701>.
- 742 [51] P. Gale, Thermodynamic equilibrium dose-response models for MERS-CoV infection reveal a
743 potential protective role of human lung mucus but not for SARS-CoV-2, *Microb Risk Anal*. 16 (2020)
744 100140–100140. <https://doi.org/10.1016/j.mran.2020.100140>.
- 745 [52] S.E. Eikenberry, M. Mancuso, E. Iboi, T. Phan, K. Eikenberry, Y. Kuang, E. Kostelich, A.B. Gumel,
746 To mask or not to mask: Modeling the potential for face mask use by the general public to curtail the
747 COVID-19 pandemic, *Infectious Disease Modelling*. 5 (2020) 293–308.
748 <https://doi.org/10.1016/j.idm.2020.04.001>.
- 749 [53] N. van Doremalen, T. Bushmaker, D.H. Morris, M.G. Holbrook, A. Gamble, B.N. Williamson, A.
750 Tamin, J.L. Harcourt, N.J. Thornburg, S.I. Gerber, J.O. Lloyd-Smith, E. de Wit, V.J. Munster, Aerosol and
751 Surface Stability of SARS-CoV-2 as Compared with SARS-CoV-1, *N Engl J Med*. 382 (2020) 1564–1567.
752 <https://doi.org/10.1056/NEJMc2004973>.
- 753 [54] W. Yang, L.C. Marr, Dynamics of Airborne Influenza A Viruses Indoors and Dependence on
754 Humidity, *PLOS ONE*. 6 (2011) e21481. <https://doi.org/10.1371/journal.pone.0021481>.

- 755 [55] S.E. Chatoutsidou, M. Lazaridis, Assessment of the impact of particulate dry deposition on
756 soiling of indoor cultural heritage objects found in churches and museums/libraries, *Journal of*
757 *Cultural Heritage*. 39 (2019) 221–228. <https://doi.org/10.1016/j.culher.2019.02.017>.
- 758 [56] L. Stabile, M. Dell'Isola, A. Russi, A. Massimo, G. Buonanno, The effect of natural ventilation
759 strategy on indoor air quality in schools, *Science of the Total Environment*. 595 (2017) 894–902.
760 <https://doi.org/10.1016/j.scitotenv.2017.02.030>.
- 761 [57] F.R. d'Ambrosio Alfano, M. Dell'Isola, G. Ficco, F. Tassini, Experimental analysis of air tightness
762 in Mediterranean buildings using the fan pressurization method, *Building and Environment*. 53 (2012)
763 16–25. <https://doi.org/10.1016/j.buildenv.2011.12.017>.
- 764 [58] L. Stabile, M. Dell'Isola, A. Frattolillo, A. Massimo, A. Russi, Effect of natural ventilation and
765 manual airing on indoor air quality in naturally ventilated Italian classrooms, *Building and*
766 *Environment*. 98 (2016) 180–189. <https://doi.org/10.1016/j.buildenv.2016.01.009>.
- 767 [59] C. Howard-Reed, L.A. Wallace, W.R. Ott, The Effect of Opening Windows on Air Change Rates in
768 Two Homes, *Journal of the Air & Waste Management Association*. 52 (2002) 147–159.
769 <https://doi.org/10.1080/10473289.2002.10470775>.
- 770 [60] L. Stabile, A. Massimo, L. Canale, A. Russi, A. Andrade, M. Dell'Isola, The Effect of Ventilation
771 Strategies on Indoor Air Quality and Energy Consumptions in Classrooms, *Buildings*. 9 (2019).
772 <https://doi.org/10.3390/buildings9050110>.
- 773 [61] L. Canale, M. Dell'Isola, G. Ficco, B. Di Pietra, A. Frattolillo, Estimating the impact of heat
774 accounting on Italian residential energy consumption in different scenarios, *Energy and Buildings*. 168
775 (2018) 385–398. <https://doi.org/10.1016/j.enbuild.2018.03.040>.
- 776 [62] M. Dell'Isola, G. Ficco, F. Arpino, G. Cortellessa, L. Canale, A novel model for the evaluation of
777 heat accounting systems reliability in residential buildings, *Energy and Buildings*. 150 (2017) 281–
778 293. <https://doi.org/10.1016/j.enbuild.2017.06.007>.
- 779 [63] M. Dell'Isola, G. Ficco, L. Canale, B.I. Palella, G. Puglisi, An IoT Integrated Tool to Enhance User
780 Awareness on Energy Consumption in Residential Buildings, *Atmosphere*. 10 (2019).
781 <https://doi.org/10.3390/atmos10120743>.
- 782 [64] L. Canale, M. Dell'Isola, G. Ficco, T. Cholewa, S. Siggele, I. Balen, A comprehensive review on
783 heat accounting and cost allocation in residential buildings in EU, *Energy and Buildings*. 202 (2019)
784 109398. <https://doi.org/10.1016/j.enbuild.2019.109398>.
- 785 [65] A. Heebøll, P. Wargocki, J. Toftum, Window and door opening behavior, carbon dioxide
786 concentration, temperature, and energy use during the heating season in classrooms with different
787 ventilation retrofits—ASHRAE RP1624, *Science and Technology for the Built Environment*. 24 (2018)
788 626–637. <https://doi.org/10.1080/23744731.2018.1432938>.
- 789 [66] S. Cui, M. Cohen, P. Stabat, D. Marchio, CO₂ tracer gas concentration decay method for
790 measuring air change rate, *Building and Environment*. 84 (2015) 162–169.
791 <https://doi.org/10.1016/j.buildenv.2014.11.007>.
- 792 [67] M. Abbas, D. Pittet, Surfing the COVID-19 scientific wave, *Lancet Infect Dis.* (2020) S1473-
793 3099(20)30558–2. [https://doi.org/10.1016/S1473-3099\(20\)30558-2](https://doi.org/10.1016/S1473-3099(20)30558-2).
- 794 [68] C. Alteri, V. Cento, A. Piralla, V. Costabile, M. Tallarita, L. Colagrossi, S. Renica, F. Giardina, F.
795 Novazzi, S. Gaiarsa, E. Matarazzo, M. Antonello, C. Vismara, R. Fumagalli, O.M. Epis, M. Puoti, C.F. Perno,
796 F. Baldanti, Genomic epidemiology of SARS-CoV-2 reveals multiple lineages and early spread of SARS-
797 CoV-2 infections in Lombardy, Italy, *Nature Communications*. 12 (2021) 434.
798 <https://doi.org/10.1038/s41467-020-20688-x>.
- 799 [69] A.C. Fears, W.B. Klimstra, P. Duprex, A. Hartman, S.C. Weaver, K.C. Plante, D. Mirchandani, J.A.
800 Plante, P.V. Aguilar, D. Fernández, A. Nalca, A. Totura, D. Dyer, B. Kearney, M. Lackemeyer, J.K.
801 Bohannon, R. Johnson, R.F. Garry, D.S. Reed, C.J. Roy, Comparative dynamic aerosol efficiencies of three

802 emergent coronaviruses and the unusual persistence of SARS-CoV-2 in aerosol suspensions, MedRxiv.
803 (2020) 2020.04.13.20063784. <https://doi.org/10.1101/2020.04.13.20063784>.

804 [70] D.W. Layton, Metabolically consistent breathing rates for use in dose assessments., Health
805 Phys. 64 (1993) 23–36. <https://doi.org/10.1097/00004032-199301000-00003>.

806 [71] L.B. Mendes, N.W.M. Ogink, N. Edouard, H.J.C. van Dooren, I. de F.F. Tinôco, J. Mosquera, NDIR
807 Gas Sensor for Spatial Monitoring of Carbon Dioxide Concentrations in Naturally Ventilated Livestock
808 Buildings, Sensors (Basel). 15 (2015) 11239–11257. <https://doi.org/10.3390/s150511239>.

809 [72] M.H. Sherman, I.S. Walker, M.M. Lunden, Uncertainties in Air Exchange using Continuous-
810 Injection, Long-Term Sampling Tracer-Gas Methods, Null. 13 (2014) 13–28.
811 <https://doi.org/10.1080/14733315.2014.11684034>.

812 [73] G. Remion, B. Moujalled, M. El Mankibi, Review of tracer gas-based methods for the
813 characterization of natural ventilation performance: Comparative analysis of their accuracy, Building
814 and Environment. 160 (2019) 106180. <https://doi.org/10.1016/j.buildenv.2019.106180>.

815 [74] A. Kabirikopaei, J. Lau, Uncertainty analysis of various CO₂-Based tracer-gas methods for
816 estimating seasonal ventilation rates in classrooms with different mechanical systems, Building and
817 Environment. 179 (2020) 107003. <https://doi.org/10.1016/j.buildenv.2020.107003>.

818

819